Improvement of Thermoelectric Performance for Sb-Doped SnO$_2$ Ceramics Material by Addition of Cu as Sintering Additive

TOSHIKI TSUBOTA,[1,2] SHOGO KOBAYASHI,[1] NAOYA MURAKAMI,[1] and TERUHISA OHNO[1]

1.—Department of Applied Chemistry, Faculty of Engineering, Kyushu Institute of Technology, 1-1 Sensuicho, Tobata-ku, Kitakyushu 804-8550, Japan. 2.—e-mail: tsubota@che.kyutech.ac.jp

The thermoelectric properties, such as the Seebeck coefficient value, S, electrical conductivity, σ, and thermal conductivity, κ, of Sb- and Cu-doped SnO$_2$, that is, $(Sn_{1-x-y}Cu_xSb_y)O_2$, were investigated in detail. The addition of a small amount of CuO significantly improved the relative density of the SnO$_2$ ceramics. However, the relative density slightly decreased with the excessive addition of CuO (more than $x = 0.03$). The addition of Sb$_2$O$_5$ should cause an increase in the number of charge carriers, resulting in an increased σ value, and the addition of both CuO and Sb$_2$O$_5$ caused an increase in σ and $|S|$ at high temperature. The improvement of the sintering performance caused the enhancement of the thermoelectric performance. As the temperature region measured in this study (293–1073 K), the maximum ZT value was 0.29 at 1073 K for $(Sn_{0.985}Cu_{0.005}Sb_{0.01})O_2$.

INTRODUCTION

The thermoelectric phenomenon is valuable for the conversion of waste heat to electrical energy. Moreover, the thermoelectric conversion has high durability because there are no moving parts. However, the conventional thermoelectric materials have a low conversion efficiency. Therefore, the application of thermoelectric conversion is limited. The performance of the thermoelectric materials is estimated by the figure of merit, Z, which is expressed by the following equation:

$$Z = S^2\sigma/\kappa, \qquad (1)$$

where S is the Seebeck coefficient, σ is the electrical conductivity, and κ is the thermal conductivity.

Metal oxides should be advantageous for high-temperature thermoelectric applications because of their high thermal stability and excellent oxidation resistance. Therefore, oxides have recently been

considered as candidates for thermoelectric material.[1] The thermoelectric properties of several oxides, such as ZnO,[2–6] NaCo$_2$O$_4$,[7–9] Li-doped NiO,[10] SrTiO3,[11,12] and Ca$_3$Co$_4$O$_9$,[13] have been studied in detail.

Tin oxide, SnO$_2$, is known as an electroconductive oxide, and is used as one of the base materials of chemical sensors. It is known that the carrier mobility of SnO$_2$ as an oxide is high. Moreover, it is reported that the carrier concentration of SnO$_2$ increases by the addition of Sb$_2$O$_5$. Titanium oxide, TiO$_2$, can dissolve in SnO$_2$. In order to decrease the thermal conductivity, we have used TiO$_2$ and studied the $(Sn_{1-x-y}Ti_xSb_y)O_2$ system.[14] Yanagiya et al.[15] have reported on the thermoelectric performance of the $(Sn_{1-x-y}Zn_xSb_y)O_2$ system, although there were no data about the thermal conductivity and the figure of merit. However, the performance of the $(Sn_{1-x-y}Ti_xSb_y)O_2$ system was insufficient as a thermoelectric material. In general, SnO$_2$ ceramics have a porous structure. The thermoelectric performance of the SnO$_2$ system could be improved with a dense structure because the value of the electrical conductivity should be significantly improved. It is
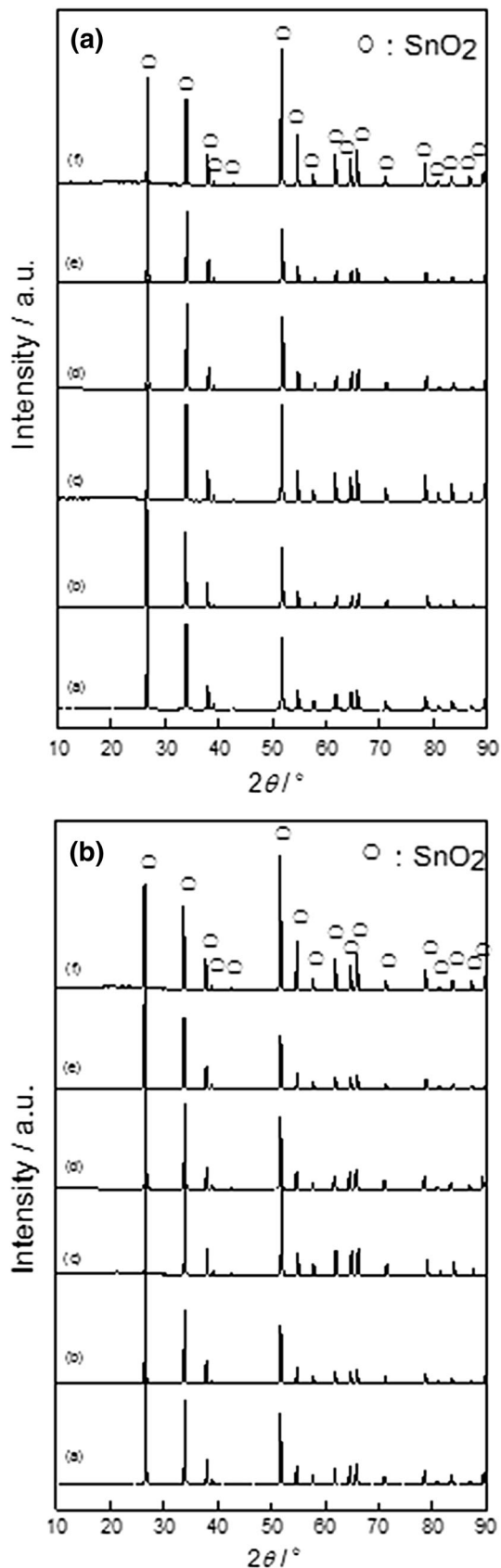
Fig. 1. XRD patterns of $(Sn_{1-x-y}Cu_xSb_y)O_2$. (A) $y = 0.01$; (B) $y = 0.02$; (a), $x = 0.0025$; (b), $x = 0.005$; (c), $x = 0.0075$; (d), $x = 0.01$; (e), $x = 0.03$; (f), $x = 0.05$.
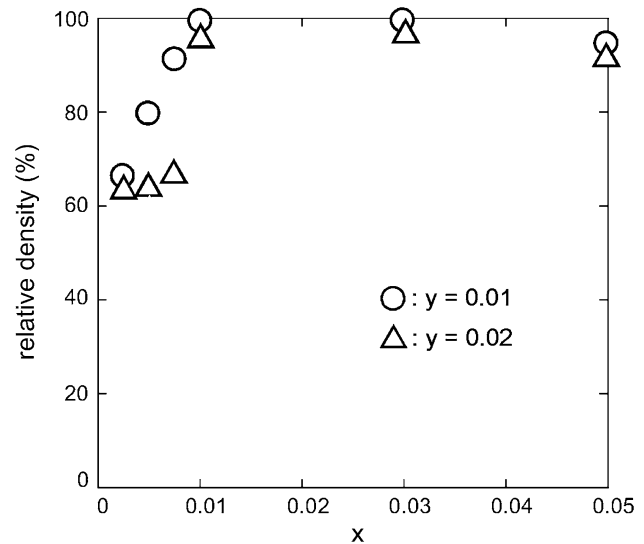

Fig. 2. The relative density of $(Sn_{1-x-y}Cu_xSb_y)O_2$.

reported that the addition of CuO improves the sintering property of SnO_2.[16] Therefore, in this study, we investigated the addition of both Cu and Sb to SnO_2, i.e., the $(Sn_{1-x-y}Cu_xSb_y)O_2$ system.

EXPERIMENTAL

Samples of $(Sn_{1-x-y}Cu_xSb_y)O_2$ ceramics were prepared from the fine powders of SnO_2, CuO, and Sb_2O_5. Properly weighed powders were mixed in a nylon-line ball mill for 24 h, and then pressed into pellets at a pressure of 50 MPa at room temperature. The pellets were heated at 1300°C for 10 h in air.

The crystal phases in the samples were examined by a powder x-ray diffraction (XRD) study. The electrical measurements were carried out using the samples cut from the sintered pellets as parallelepiped bars of ca. 4 mm 3 mm 15 mm in size. The electrical conductivities and the Seebeck coefficients were measured using an ULVAC ZEM-1 instrument in a helium atmosphere. The electrical conductivities were measured by a DC four-probe technique and the Seebeck coefficients were simultaneously measured with temperature gradients of 5–30 K over the samples. The thermal conductivities were evaluated from the thermal diffusivity D, the heat capacity C_p, and the experimental density d, using the following relationship:

$$\kappa = DC_pd \qquad (2)$$

The thermal diffusivities were measured by a laser flash method using an ULVAC TC-7000 instrument in vacuum. The heat capacitances were also measured by the laser flash method using an ULVAC TC-7000 instrument in a vacuum using the measured absorbed duty, the density of the sample, and the change in temperature. The figure of merit
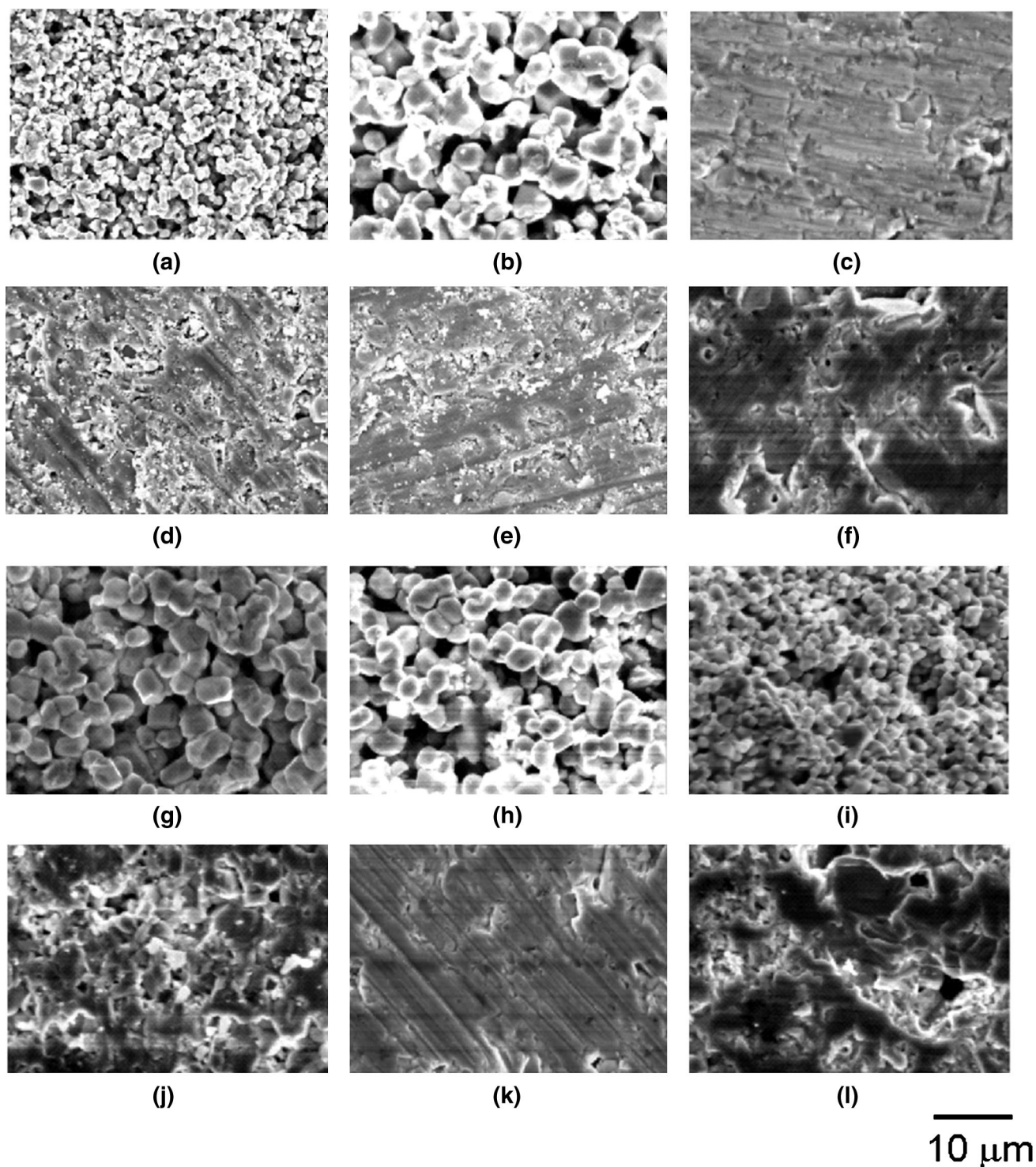
Improvement of Thermoelectric Performance for Sb-Doped SnO$_2$ Ceramics Material
by Addition of Cu as Sintering Additive

3569

Fig. 3. SEM images of (Sn$_{1-x-y}$Cu$_x$Sb$_y$)O$_2$. (a–f) $y = 0.01$; (g–l) $y = 0.02$; (a, g) $x = 0.0025$; (b, h) $x = 0.005$; (c, i) $x = 0.0075$; (d, j) $x = 0.01$; (e, k) $x = 0.03$; (f, l) $x = 0.05$.

was calculated from the above-mentioned values. Microstructure observations were carried out using a digital scanning electron microscope (SEM). The relative density of the sintered samples was determined by Archimedes's method.

RESULTS AND DISCUSSION

The XRD measurements were performed on the (Sn$_{1-x-y}$Cu$_x$Sb$_y$)O$_2$ sample. The XRD patterns of the samples indicated that the crystal structures of all
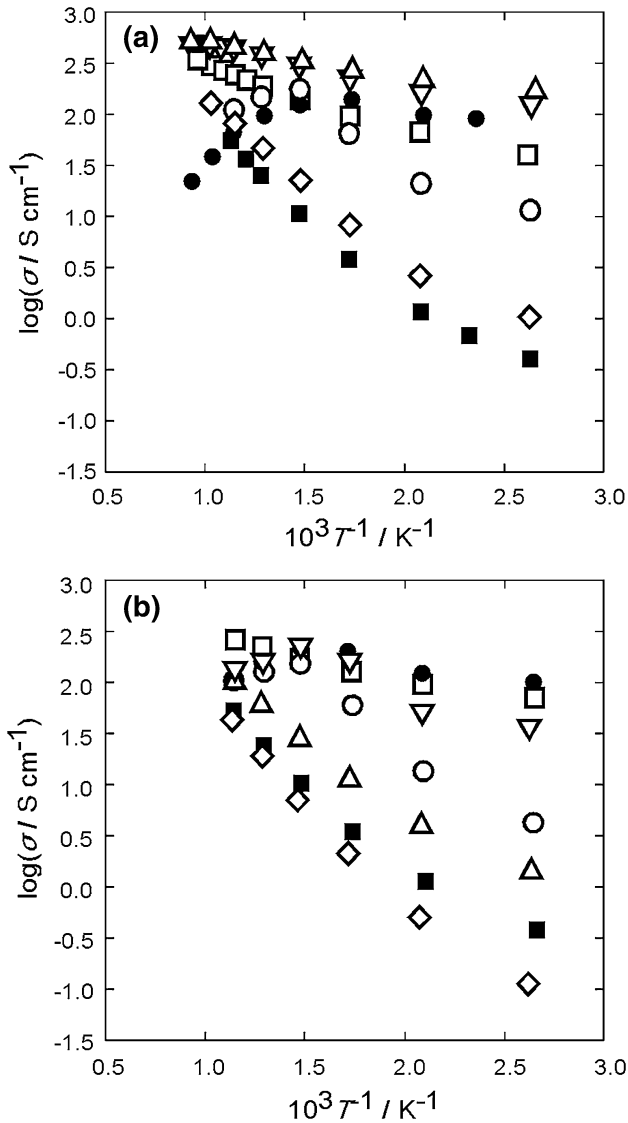
Fig. 4. Arrhenius plots of electrical conductivity of $(Sn_{1-x-y}Cu_xSb_y)O_2$. (a) $y = 0.01$; (b) $y = 0.02$. ● $x = 0$, ○ $x = 0.0025$, ▽ $x = 0.005$, △ $x = 0.0075$, □ $x = 0.01$, ◇ $x = 0.03$, ■ $x = 0.05$.

Fig. 5. Seebeck coefficients of $(Sn_{1-x-y}Cu_xSb_y)O_2$ as a function of temperature. (a) $y = 0.01$; (b) $y = 0.02$. ● $x = 0$, ○ $x = 0.0025$, ▽ $x = 0.005$, △ $x = 0.0075$, □ $x = 0.01$, ◇ $x = 0.03$, ■ $x = 0.05$.

the samples were assigned to the SnO_2 phase (Fig. 1). These experimental results could mean that both Sb_2O_5 and CuO had dissolved in the SnO_2 phase. However, the peaks related to the generated impurity phase might not be detected because the amounts of the added additives were low. Therefore, there was the possibility that a small part of the additives segregate at the grain boundary.

Figure 2 shows the relative density of the sample of $(Sn_{1-x-y}Cu_xSb_y)O_2$, from which it was confirmed that the addition of CuO drastically improved the relative density of the SnO_2 ceramics, although the addition of Sb slightly suppressed the sintering performance. Because the added CuO must affect the surface energy of the SnO_2 grains, at least part of the added CuO should exist at the grain boundary. It is known that Sb_2O_5 dissolves in Sb_2O_3 at
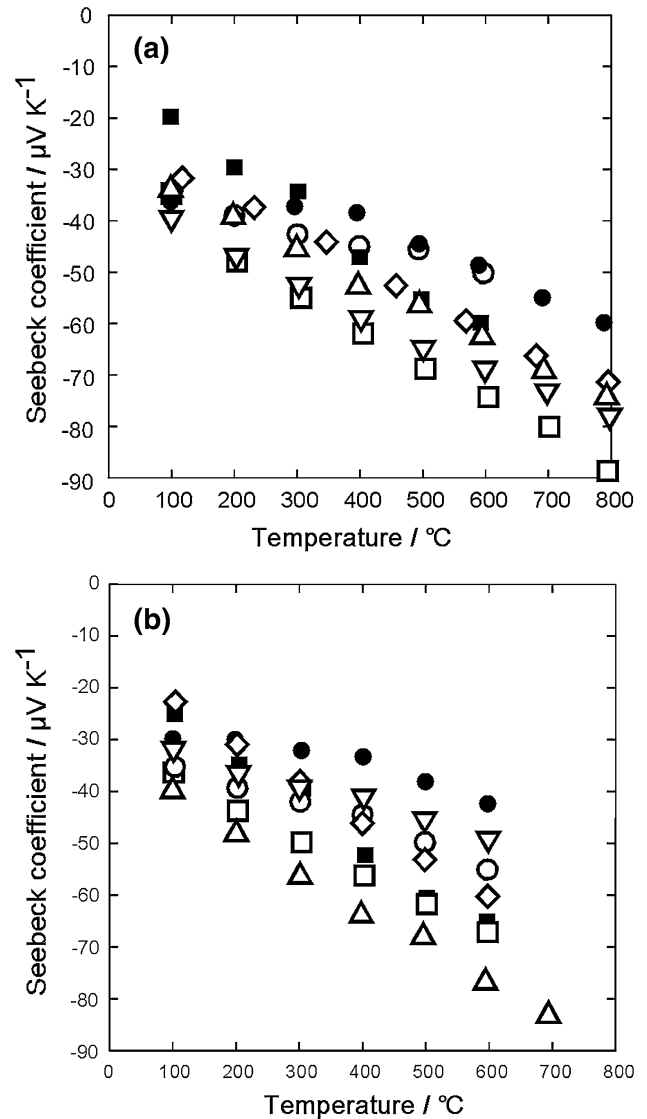
ca. 900°C with outgassing. The boiling point of Sb_2O_5 is 1425°C. Therefore, the suppression of the relative density should be caused by the gaseous product and/or the disappearance of Sb_2O_5 during the heating process. Moreover, the relative density slightly decreased with the excessive addition of CuO (more than $x = 0.01$).

The SEM images of the samples are shown in Fig. 3. The SEM images also indicated that the addition of CuO is effective for improving of the sintering performance of the SnO_2 matrix. In the case of the samples of $y = 0.01$, the grain size increased with the increasing amount of added CuO up to $x = 0.0075$. The samples of $x \geq 0.01$ had many voids between the grains. The generation of the voids should be the reason for the slight decrease in the relative density in the range of the excessive
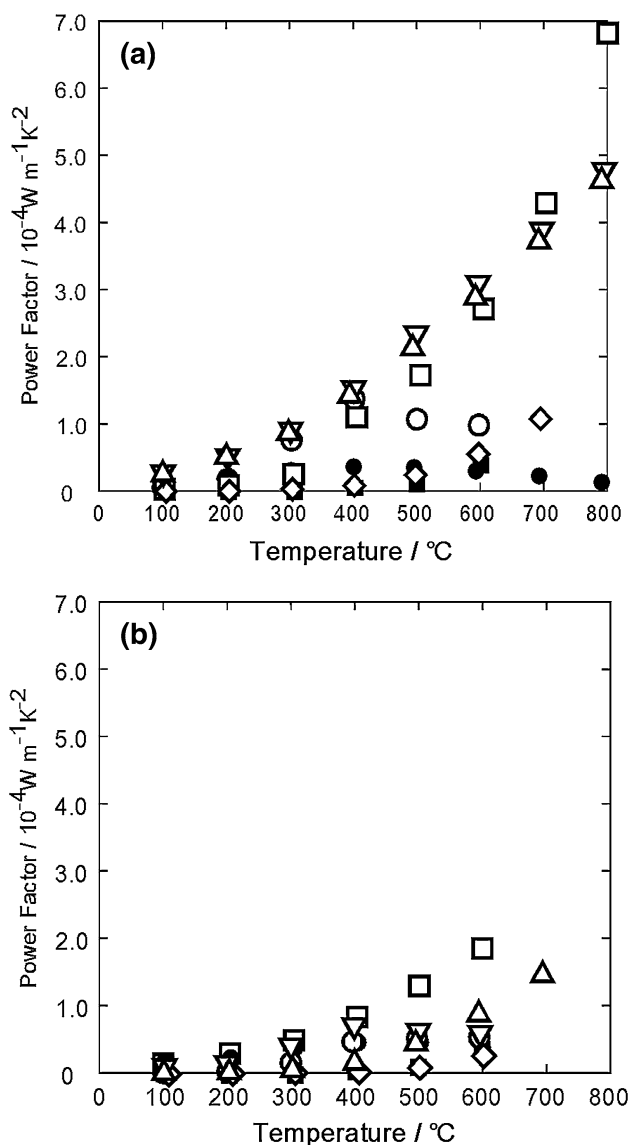
Improvement of Thermoelectric Performance for Sb-Doped SnO$_2$ Ceramics Material by Addition of Cu as Sintering Additive

3571

(a)

Fig. 7. Thermal conductivity of $(Sn_{1-x-y}Cu_xSb_y)O_2$ at room temperature (25°C).

(b)

Fig. 6. Power Factor of $(Sn_{1-x-y}Cu_xSb_y)O_2$ as a function of temperature. (a) $y = 0.01$; (b) $y = 0.02$. ● $x = 0$, ○ $x = 0.0025$, ▽ $x = 0.005$, △ $x = 0.0075$, □ $x = 0.01$, ◇ $x = 0.03$, ■ $x = 0.05$.

addition of CuO. On the other hand, in the case of $y = 0.02$, the grain size decreased with the increasing amount of added CuO up to $x = 0.0075$. The gaseous product derived from Sb$_2$O$_5$ and/or the disappearance of Sb$_2$O$_5$ during the heating process may be the reason for the decrease in the grain size.

Arrhenius plots of the electric conductivity values, σ, for the samples are shown in Fig. 4. As shown in Fig. 4, the temperature dependence of the σ value for the sample with no added CuO had a metallic behavior, that is, the σ value decreased with the increasing temperature. On the other hand, the samples with added CuO had a semiconductive behavior, that is, the σ value increased with the increasing temperature. The high σ value of the Sb-doped sample should be explained by the theory of valence control. The reason for the metallic
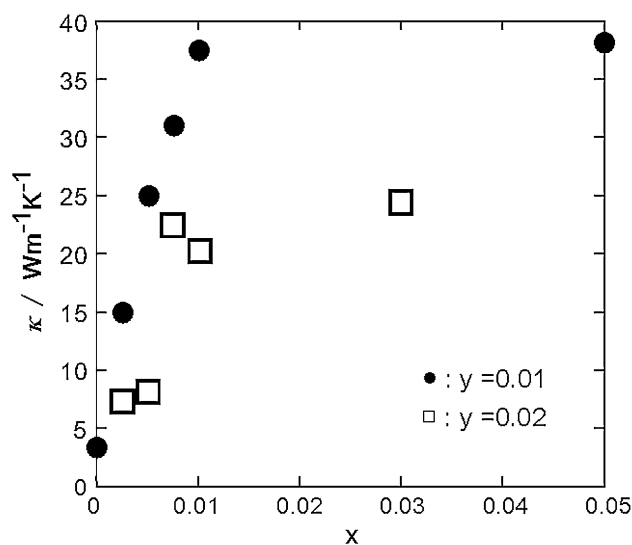
behavior of the sample with no added CuO could be a degenerated semiconductor having a high charge carrier concentration derived from Sb. The reason for the semiconductive behavior of the sample with added CuO could be suppression of the charge carrier concentration explained by the theory of valence control. That is, part of the added Cu dissolves into the SnO$_2$ matrix, and then the generated electrons derived from Sb were suppressed because the valence number of Cu should be 2. The maximum σ values was achieved at $x = 0.0075$ for $(Sn_{0.99-x}Cu_xSb_{0.01})O_2$ and at $x = 0.01$ for $(Sn_{0.98-x}Cu_xSb_{0.02})O_2$. The x values for the maximum σ values should be related to the relative density explained in Figs. 2 and 3. It is presumed that the dense structure was at least one of the reasons for the maximum σ values. Excess CuO addition caused a decrease in σ. The Cu atoms dissolved into SnO$_2$ should act as the carrier scattering center. Moreover, the CuO-related phase at the grain boundary should act as the carrier scattering center. The decrease in σ, therefore, would be caused by the decrease in the carrier mobility. The relative densities were a maximum at $x = 0.03$ as shown in Fig. 2. The SEM images shown in Fig. 3 agree with the tendency of the relative density. That is, the density of pores decreased with increasing the x value up to $x = 0.03$, and then that increased with increasing the x value more than $x = 0.03$. Wang et al. reported the sintering property of the CuO-Ta$_2$O$_5$-SnO$_2$ system.[17] The relative density of the samples increased when the amount of the added CuO was low, whereas that of the samples decreased with the excessive addition of CuO. The reason for the improvement of the density should be the formation of oxygen vacancies.[18] Wang et al. considered that the suppression of the density with the excessive addition of CuO could be explained by the evaporation of copper oxide because the melting point of
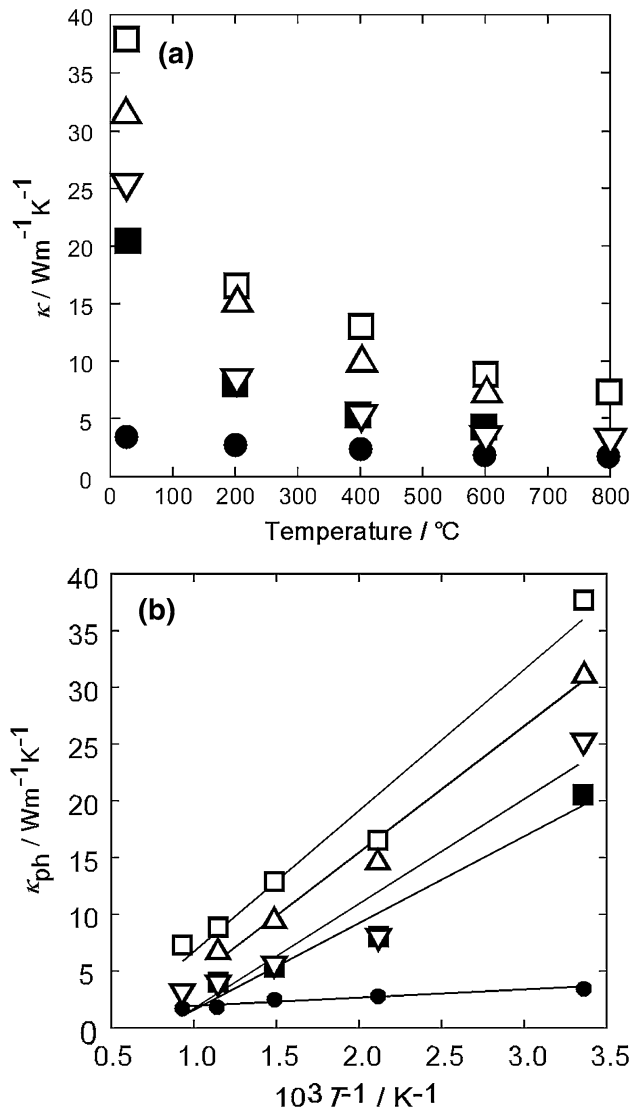
Fig. 8. (a) Thermal conductivity of $(Sn_{1-x-y}Cu_xSb_y)O_2$ as a function of temperature. (b) Lattice thermal conductivity of $(Sn_{1-x-y}Cu_xSb_y)O_2$ as a function of temperature. ● $x = 0$. $y = 0.01$; ▽ $x = 0.005$, $y = 0.01$; △ $x = 0.0075$, $y = 0.01$; □ $x = 0.01$, $y = 0.01$; ■ $x = 0.01$, $y = 0.02$.

Fig. 9. Dimensionless figure of merit of $(Sn_{1-x-y}Cu_xSb_y)O_2$ as a function of temperature. ● $x = 0$. $y = 0.01$; ▽ $x = 0.005$, $y = 0.01$; △ $x = 0.0075$, $y = 0.01$; □ $x = 0.01$, $y = 0.01$; ■ $x = 0.01$, $y = 0.02$.

Cu_2O (1236°C), which could be generated from CuO at 1122°C, is lower than the sintering temperature (1300°C). The maximum relative density appeared at $x = 0.25$ in the study of Wang et al., whereas it appeared at $x = 0.01$ in this study. The reason for the difference in the x value for the maximum density could be the difference in the third components, that is, Ta_2O_5 or Sb_2O_5. However, the mechanisms for the improvement of the sintering and the suppression of the sintering for the samples of this study should be the same as those for the samples reported by Wang et al.

The Seebeck coefficients of $(Sn_{1-x-y}Cu_xSb_y)O_2$ are shown in Fig. 5. The signs of the Seebeck coefficient were negative for all samples, indicating that all the samples were n-type conductors. As shown in Fig. 5, the absolute values of the Seebeck coefficient, $|S|$,
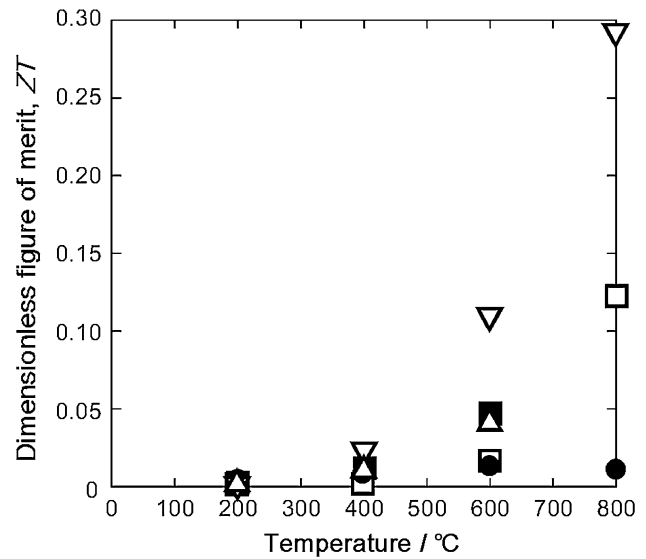
for the samples increased with the increasing temperature. All the samples doped with CuO had a higher $|S|$ value than the no-CuO-added samples. However, the excessive addition of CuO [more than 0.01 ($y = 0.01$), more than 0.0075 ($y = 0.02$)] caused a decrease in the $|S|$ value. The maximum $|S|$ values were achieved at $x = 0.01$ in the case of $(Sn_{0.99-x}Cu_xSb_{0.01})O_2$ and at $x = 0.0075$ in the case of $(Sn_{0.98-x}Cu_xSb_{0.02})O_2$. These x values are similar to the x values for the highest relative density and for the maximum σ values. Considering band theory, the following equations can be derived,

$$\sigma = n e \mu \tag{3}$$

$$S = -(k/e)[\ln(N_v/n) + A], \tag{4}$$

where n is the carrier concentration, e is the electric charge of the carrier, μ is the carrier mobility, k is the Bolzmann constant, Nv is the density of state, and A is typically a transport constant. From Eqs. 3 and 4, the increase in the carrier concentration should cause both an enhancement of σ and a decrease in $|S|$. In this study, both values increased in the case of $0 < x < 0.005$ and $0 < y < 0.02$. Therefore, the enhancement of σ should be caused not by the change in n but by the change in μ. Moreover, the n value should decrease rather than increase. The change in μ could be explained by the enhancement of the relative density. The decrease in n could be related to the substitution of Cu for Sn because the substitution should be presumed to decrease the n value because Cu is monovalent or divalent and Sn is quadrivalent. Therefore, we can consider that the improvement in the sintering performance should be the reason for the enhancement of the σ value.

The power factors, $S^2\sigma$, of the samples are shown in Fig. 6. The $S^2\sigma$ values of the sample with added CuO were higher than those of the sample with no added CuO. Especially, the $S^2\sigma$ values of the sample with added CuO increased with the increasing temperature, and the $S^2\sigma$ value of $Sn_{0.98}Cu_{0.01}Sb_{0.01}O_2$ reached ca. 7×10^{-4} W m^{-1} K^{-2}.

Figure 7 shows the thermal conductivity values for the samples at room temperature. The thermal conductivity of the samples significantly increased with the increasing amount of added CuO up to $x = 0.01$. The reason for the change in the κ value should be the improvement of the relative density. In the case of $y = 0.02$, the thermal conductivity gradually increased with the increasing x value. The κ values for the samples are very high for a thermoelectric material. Figure 8a shows the temperature dependence of the thermal conductivity. The thermal conductivity of the samples decreased with the increasing temperature. The carrier thermal conductivity was estimated from the Wiedemann–Franz law,

$$\kappa_{el} = L\sigma T, \qquad (5)$$

where L is the Lorenz number. The experimental results in this study indicated that the thermal conductivity of the $(Sn_{1-x-y}Cu_xSb_y)O_2$ system consists of a predominant proportion of the phonon thermal conductivity, κ_{ph}, which is calculated by subtracting κ_{el} from the overall κ. The calculated κ_{ph} values were proportional to the inverse of the absolute temperature as shown in Fig. 8b. This result agrees with the previously reported values.[19,20]

Figure 9 shows the temperature dependence of the figure of merit, ZT, calculated from the measured values of σ, S, and κ. The ZT values of all the samples increased with the increasing temperature. Although the ZT values of the sample with no added CuO was very low, the ZT values were significantly enhanced by the addition of CuO in the high temperature region. For the temperature region measured in this study (293–1073 K), the maximum ZT value was 0.29 at 1073 K for $(Sn_{0.985}Cu_{0.005}Sb_{0.01})O_2$. This value is comparable the reported candidates of n-type oxide thermoelectric materials.[1] Although this ZT value from this study is insufficient for practical use, the ZT value should be remarkable because the ZT value was significantly improved by the addition of CuO. Moreover, in the higher temperature region, the ZT value of the samples should increase because the ZT value of $(Sn_{1-x-y}Cu_xSb_y)O_2$ increases with the increasing temperature. The SnO_2 system should be a candidate as a thermoelectric material.

CONCLUSIONS

The thermoelectric properties of $(Sn_{1-x-y}Cu_xSb_y)O_2$ were investigated in detail. The addition of CuO significantly improved the sintering performance of the SnO_2 matrix. However, the excessive addition of CuO was ineffective for improving the sintering of SnO_2. The doping of CuO improved the σ value by improving the relative density. In the high temperature region, all samples doped with CuO had higher $|S|$ values than the no-CuO-added samples. However, the excessive addition of CuO caused a decrease in the $|S|$ value. The $S^2\sigma$ values were enhanced with the addition of CuO. The thermal conductivity value for the samples at room temperature increased with the increasing addition of CuO. The thermal conductivity values for the samples decreased with the increasing temperature. The phonon thermal conductivity was the main component of the thermal conductivity for the $(Sn_{1-x-y}Cu_xSb_y)O_2$ system. In the temperature region measured in this study, the maximum ZT value was 0.29 at 1073 K for $(Sn_{0.985}Cu_{0.005}Sb_{0.01})O_2$.

REFERENCES

1. J.W. Fergus, *J. Eur. Ceram. Soc.* 32, 525 (2012).
2. M. Ohtaki, T. Tsubota, K. Eguchi, and H. Arai, *J. Appl. Phys.* 79, 1816 (1996).
3. T. Tsubota, M. Ohtaki, K. Eguchi, and H. Arai, *J. Mater. Chem.* 7, 85 (1997).
4. H. Ohta, W.S. Seo, and K. Koumoto, *J. Am. Ceram. Soc.* 79, 2193 (1996).
5. Y. Tanaka, T. Ifuku, and K. Tsuchida, *J. Mater. Sci. Lett.* 16, 155 (1997).
6. M. Sondergaard, E.D. Bojesen, K.A. Borup, S. Christensen, M. Christensen, and B.B. Iversen, *Acta Mater.* 61, 3314 (2013).
7. I. Terasaki, Y. Sasago, and K. Uchinokura, *Phys. Rev.* B56, 12685 (1997).
8. K. Kurosaki, H. Muta, and M. Uno, *J. Alloys Compd.* 315, 234 (2001).
9. S. Tajima, T. Tani, and S. Isobe, *Mater. Sci. Eng.* B86, 20 (2001).
10. M.B. Dutt, R. Banerjee, and A.K. Barua, *Phys. Status Solidi* A65, 365 (1981).
11. L. Li, Y. Liu, X. Qin, D. Li, J. Zhang, C. Song, and L. Wang, *J. Alloys Compd.* 588, 562 (2014).
12. M.T. Buscaglia, F. Maglia, U. Anselmi-Tamburini, D. Marré, I. Pallecchid, A. Ianculescue, G. Canua, M. Viviania, M. Fabriziof, and V. Buscaglia, *J. Eur. Ceram. Soc.* 34, 307 (2014).
13. D. Kenfaui, B. Lenoir, D. Chateigner, B. Ouladdiaf, M. Gomina, and J.G. Noudem, *J. Eur. Ceram. Soc.* 32, 2405 (2012).
14. T. Tsubota, T. Ohno, N. Shiraishi, and Y. Miyazaki, *J. Alloys Compd.* 463, 288 (2008).
15. S. Yanagiya, N.V. Nong, J. Xu, M. Sonne, and N. Pryds, *J. Electron. Mater.* 40, 674 (2011).
16. N. Dolet, J.M. Heintz, L. Rabardel, M. Onillon, and J.P. Bonnet, *J. Mater. Sci.* 30, 365 (1995).
17. C.M. Wang, J.F. Wang, Y. Zhao, and W.B. Su, *J. Phys. D Appl. Phys.* 39, 1684 (2006).
18. C.M. Wang, J.F. Wang, C.L. Wang, H.C. Chen, W.B. Su, G. Z. Zang, and P. Qi, *J. Appl. Phys.* 97, 126103 (2005).
19. C.B. Vining, *J. Appl. Phys.* 69, 331 (1991).
20. G.A. Slack and M.A. Hussain, *J. Appl. Phys.* 70, 2294 (1991).